Contents lists available at ScienceDirect

Sensors and Actuators A: Physical

journal homepage: www.elsevier.com/locate/sna

A micro-robot fish with embedded SMA wire actuated flexible biomimetic fin

Zhenlong Wang [a], Guanrong Hang [a,*], Jian Li [a], Yangwei Wang [a], Kai Xiao [b]

[a] School of Mechatronics Engineering, Harbin Institute of Technology, PO Box 421, Harbin, Heilongjiang, China
[b] Department of Mechanical Engineering, The Hong Kong University of Science and Technology, Clear Water Bay, Kowloon, Hong Kong, China

ARTICLE INFO

ABSTRACT

A flexible biomimetic fin propelled micro-robot fish is presented. Fish muscle and the musculature of squid/cuttlefish fin are analyzed firstly. Since the latter one is easier to be realized in the engineering field, it is emulated by biomimetic fin. Shape memory alloy (SMA) wire is selected as the most suitable actuator of biomimetic fin. Elastic energy storage and exchange mechanism is incorporated into the biomimetic fin for efficiency improvement. Furthermore the bending experiments of biomimetic fin were carried out to verify the original ideas and research concepts. Thermal analysis is also conducted to find a proper actuation strategy. Fish swimming mechanism is reviewed as the foundation of the robot fish. A radio frequency controlled micro-robot fish propelled by biomimetic fin was built. Experimental results show that the micro-robot fish can swim straight and turn at different duty ratios and frequencies. *Subcarangiform*- and *carangiform*-like swimming modes were realized. The maximum swimming speed and the minimum turning radius reached 112 mm/s and 136 mm, respectively.

1. Introduction

Fish tail-like propeller is considered as an alternative apparatus for thrust to commonly used rotator of underwater vehicle (UV). As the propulsive efficiency of small UVs is usually below 40%, fish tail-like propeller is superior to rotator used in small UVs [1]. Another advantage of fish tail-like propeller is that the steering radius can be small even at high swimming speed. Micro-robot fish have great advantages in exploring complex, narrow underwater environments. They may even be used in blood vessels for microsurgery. Many micro-robot fish have been developed in recent years. Most reported micro-robot fish are driven by shape memory alloys (SMAs) [2,3], Ionic exchange Polymer Metal Composites (IPMCs) [4–6] or piezoelectric (PZT) actuators [7,8]. The swimming performances of some micro-robot fish were investigated. For instance, the IPMC actuated tadpole robot, which is 96 mm in length and 16.2 g in weight, reached a maximum speed of 23.6 mm/s at 4 Hz driving frequency, and the IPMC actuated micro-robot fish, which is 230 mm in length and 295 g in weight, reached a peak speed of 6.3 mm/s at 2 Hz. The difficulties of developing a micro-robot fish mainly lie in selection of actuators, sealing, compactness, wireless controlling, reducing noise and improving propulsive efficiency.

In this paper the development of a micro-robot fish driven by an embedded SMA wire actuated biomimetic fin is investigated. The flexible bending biomimetic fin simulates the musculature and flexible bending of squid/cuttlefish fin, which is supported and driven by a special skeleton—'muscular hydrostat' [9,10]. SMA wires act as 'transverse muscles' of the biomimetic fin. Elastic energy storage and exchange mechanism [11] is incorporated in the bending of the biomimetic fin. The radio frequency controlled micro-robot fish can swim straight and turn noiseless at different duty ratios and at different frequencies.

The paper is structured as follows. In Section 2, the musculature of cuttlefish fin and the structure of biomimetic fin are investigated, furthermore the bending experiments of the biomimetic fin were conducted to verify the concept. In Section 3, thermal analysis for control strategy of biomimetic fin is applied. In Section 4, the design of the micro-robot fish propelled by biomimetic fin is discussed in detail. In Section 5, straight swimming and turning capability of the micro-robot fish are investigated and discussed. Finally, the conclusions are given in Section 6.

2. Embedded SMA wire actuated flexible biomimetic fin

2.1. Musculature of cuttlefish fin

The design of propulsor is the foundation of micro-robot fish. Since evolutionary processes of millions of years have almost optimized the shape and structure of aquatic animals, it is an effective way to mimic the structure and function of fins of aquatic animals

* Corresponding author. Tel.: +86 451 86416323x601; fax: +86 451 86413485.
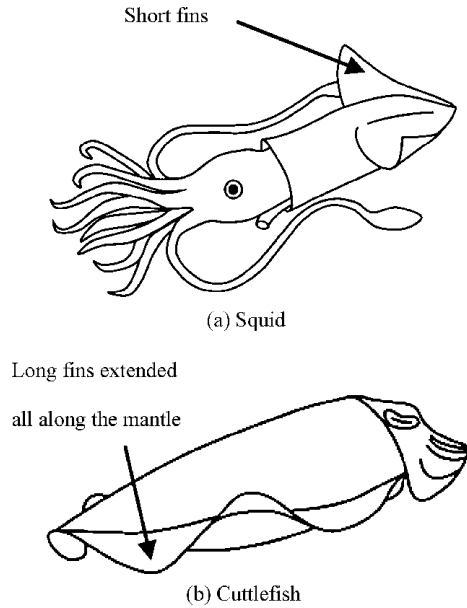E-mail address: hanggr@163.com (G. Hang).

Short fins

(a) Squid

Long fins extended

all along the mantle

(b) Cuttlefish

Fig. 1. Squid and cuttlefish.

Fig. 2. Schematic diagram of the musculature of squid/cuttlefish fin.

directly. The flexible bending fin like structure is called biomimetic fin in this paper.

Fish of body and/or caudal fin (BCF) propulsion modes bend their propulsor flexibly by activating alternate sides of W-shaped segmented muscles in sequential manner, to form a backward propulsive wave. Obviously, the most direct way to realize flexible bending is to mimic the W shaped muscles, connective tissue and bones by using artificial materials. However, it is difficult to realize this structure because of the complexity of segmented arranged W shaped muscles, especially for micro-robot fish.

Besides fish, another two kinds of aquatic animals with excellent swimming capability are squid and cuttlefish (shown in Fig. 1), which belong to Cephalopoda. Squid and cuttlefish swim by using a combination of jet propulsion at high speed and fin undulatory/oscillatory propulsion at low speed [12,13]. Squid fins are short while cuttlefish fins are long, however their structures are similar. Therefore, the cuttlefish fin structure is selected for explanation. The frill-like cuttlefish fins extend all along the mantle and they can bend flexible into an undulatory motion for propulsion. If a short segment of cuttlefish fin is taken, the movement is flexible bending upward and downward only, which is similar to the movement of fish. So the muscular structure of cuttlefish fin is worthy to be investigated to realize flexible bending. The cuttlefish fins consist of a tightly packed 3-dimensional array of musculature called 'muscular hydrostat', which can generate force and support movement without bony skeleton support or fluid-filled cavities for hydrostatic skeletal support.

Fig. 2 shows the muscular structure of cuttlefish fin. The fin extends from fin cartilage (FC). The median connective tissue fascia (MF) divided the fin into two similar parts: dorsal part and ventral part. Transverse muscle fibers (T) extend parallel to the fin surface from the fin base to the fin margin, some of them insert on MF. Dorsalventral muscle fibers (DV) extend from dorsal and ventral connective tissue fascia (DF and VF) to MF. Longitudinal muscle fibers (L) lie adjacent to both the dorsal and ventral surface of MF. The connective tissue fibers (CT), which are oriented at 45° to the long axes of T and DV, are presented among the T and DV. L and DV control the length and thickness of the fin, respectively. Transverse muscle fibers control the curvature of the fin, namely lets the fin bend. CT provides skeletal support. There is little fluid into
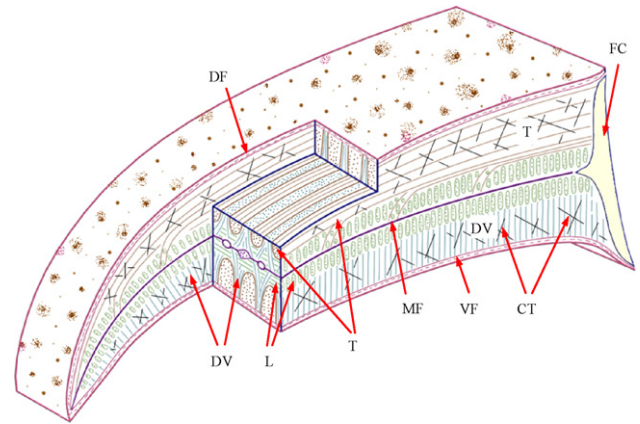
or out of the fin and there are no compressible gas-filled cavities in the fin, so the fin volume almost remains constant. When the transverse muscle fibers of dorsal part and ventral part contract and relax in sequence, the fin is laterally compressed and can bend dorsally and ventrally. During bending, connective tissue fibers provide resistance to prevent the fin contracting wholly, and they may store elastic energy together with skin and other muscles. During the subsequent motion of unbending, the stored elastic energy is released to support the movement. The elastic energy storage and exchange mechanism, which can increase efficiency and improve locomotor performance, is also commonly existed in other animals. There are two kinds of transverse muscle fibers: aerobic and anaerobic fibers. The former one is for gentle movements while the latter one is for vigorous fin movements.

2.2. Structure of biomimetic fin

To realize flexible bending by emulate the structure of a short segment of cuttlefish fin, some simplifications must be done. When the fin segment is short enough, dorsalventral and longitudinal fibers can be neglected. Then the problem turns to find proper actuators to imitate the transverse muscle fibers. Motors, PZT and IPMCs are apparently not suitable. SMA is the alloy being able to return to a predetermined shape and it can be processed into wires. The most sophisticated SMA is TiNi, the advantages of which are noiseless actuation, large recovery strain (<8%), high recovery stress (>500 MPa) [14], low actuation voltage, operational frequency similar to that of animal muscles, long life (up to 10^6 action cycles under a strain of 1%) [15]. The efficiency of SMA is low, but it is not a primary concern for the prototype. When SMA wire is thin, the activated electric value is similar to that of small DC motors. These considerations determined our choice of thin SMA wires as the most suited actuator to mimic the transverse muscle fibers. In the stress-free state, the four transition temperatures are Martensite Finish (M_f), Martensite Start (M_s), Austenite Start (A_s) and Austenite Finish (A_f).

Fig. 3 shows the structure and bending movement of biomimetic fin. Elastic substrate divides the biomimetic fin into two symmetric parts. Skins are adhered to elastic substrate, one or more SMA wires are embedded in the skin, lying adjacent to both sides of the elastic substrate. The materials for elastic substrate and skins are plastic and rubber/silicone, respectively. SMA wires serve as 'transverse muscle fibers', providing lateral compressing force. Elastic substrate is used to provide resistance and store elastic energy together with the skins. When the SMA wires of two sides are resistant heated by pulse and cooled alternatively in sequence, the biomimetic fin can
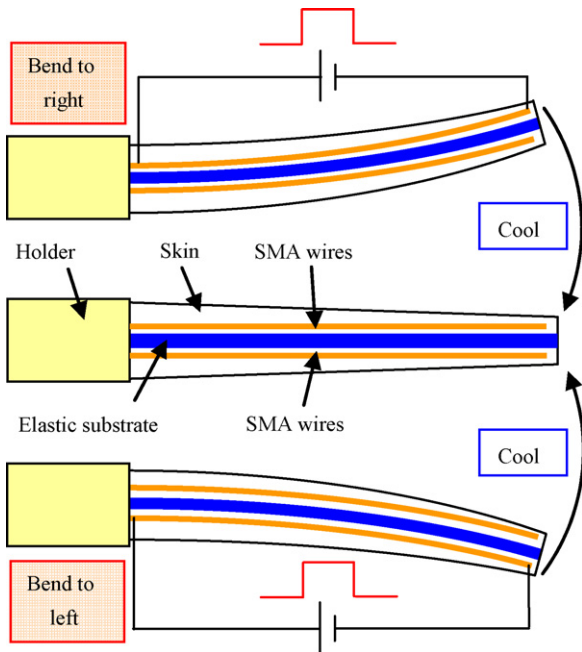
Fig. 3. The structure and the schematic of bending movement of biomimetic fin.

bend to both sides flexibly. During the process of bending movements, elastic energy is stored and relaxed just like it does during the movements of real fin. The stored elastic energy during bending is the key issue since it is the energy to let the biomimetic fin return to the straight state. Fish caudal fin like component can be attached at the tip of the biomimetic fin to enlarge control surface and thrust.

2.3. Initial experiments of bending

A biomimetic fin was built and tested in water environment to validate the concept. Table 1 illustrates the specifications of the biomimetic fin. TiNi (52 at% Ni) SMA wires are employed. In the stress-free state, the four transition temperatures are $M_f = 25.90\,^{\circ}$C, $M_s = 32.71\,^{\circ}$C, $A_s = 57.60\,^{\circ}$C, $A_f = 60.64\,^{\circ}$C, respectively. The materials for substrate and skin are polypropylene and silicone, respectively. The temperature of water (T_0) was 21 °C. The voltage and pulse width of the pulse are detonated by U and t_{on}, respectively. The two kinds of pulse sequences employed were (1) $U = 4.7$ V, $t_{on} = 0.5$ s and (2) $U = 11.0$ V, $t_{on} = 0.06$ s. After each pulse of the pulse sequence, an interval of 1.8 s was added to cool the SMA wires prior to the heating of the antagonistic SMA wires. Fig. 4 shows the curves of pulse width, bending angle and return time of the biomimetic fin activated by the two kinds of pulses. The angle of first bending of each bending sequence is defined as positive value. Fig. 5 shows the status of maximum bending angles to both sides. Over 90° of maximum bending angles to both sides were obtained. Experimental results show that the biomimetic fin can bend flexibly to both sides. When this biomimetic fin was activated by pulse

Table 1
Specifications of biomimetic fin for initial experiments

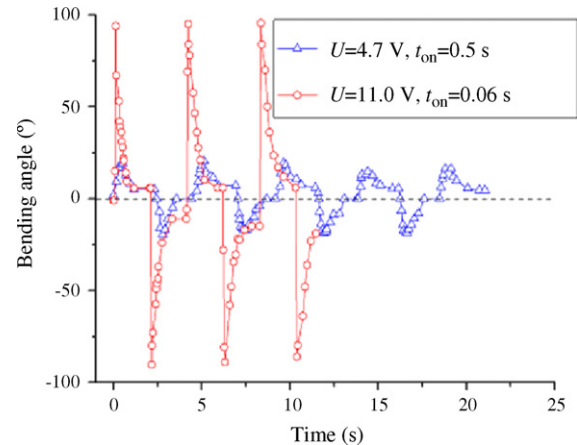|	
Width (mm)	14
Diameter of SMA wire (mm)	0.2
Length of SMA wire (mm)	48
Numbers of SMA wires	2
Length of bending segment (mm)	50
Thickness of the skin (mm)	0.6–0.7
Thickness of the substrate (mm)	0.36

Fig. 4. Experimental results of bending of biomimetic fin.

sequence (1), small bending angle was obtained even using long pulse width. This indicates that the temperature of SMA arises slowly with light electric current. When the biomimetic fin was activated by pulse sequence (2), the bending speed was much higher and large maximum bending angle could be obtained in very short time. The return speed was lower than the corresponding bending speed in experiments. In accordance to the experimental results, we know that short pulse with heavy current could be applied to activate the biomimetic fin in order to achieve high frequency actuation, and the return speed would restrict the bending frequency of the biomimetic fin driven by the Ø 0.2 mm TiNi wires.

3. Theory analysis of the biomimetic fin

Since shape memory effect is induced by temperature, heating speed and cooling speed are the major influencing factors. SMA wires are embedding in the skin, so the temperature of SMA wires is difficult to measure directly. Therefore, the thermal analysis is used to estimate the temperature of SMA wires and to find proper actuation strategy.

In order to simplify the analysis, several simplifications are made: (1) radiation effect is ignored; (2) there is no heat transfer between SMA wires and elastic substrate; (3) the skin is simplified as heat sink of SMA wires, so heat convection is considered as the only way of heat transformation, an equivalent heat transmission coefficient, h'_W (W/(m^2 K)), is used to replace the original heat transmission coefficient; (4) h'_W, specific electric resistance ρ_e (Ω m) and specific heat c (J/(kg K)) are assumed to be constant.

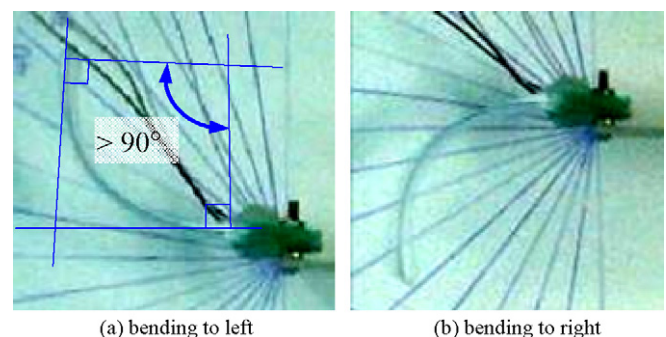**Fig. 5.** Maximum bending angles of biomimetic fin.

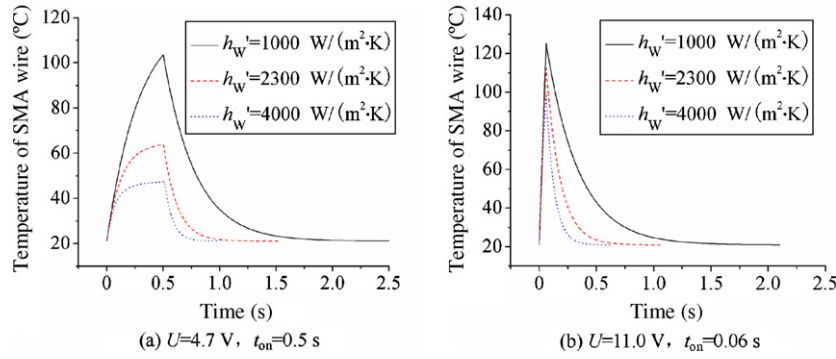(a) U=4.7 V，t_{on}=0.5 s   (b) U=11.0 V，t_{on}=0.06 s

Fig. 6. Simulation curves of the biomimetic fin used in Section 2.3.

When SMA wires are heated, the equation describing the energy input, heat transfer and the temperature of SMA wires is given as:

$$\int_t \frac{\pi d^2}{4\rho_e l} U(t)^2\, dt = \int_t h'_W \pi\, dl[T(t) - T_0]\, dt + \int_t c\rho \left(\frac{\pi d^2}{4}\right) l\, dT(t) \tag{1}$$

where $U(t)$ is the voltage supplied to SMA wires (V), d is the diameter of SMA wires (m), l is the total length of SMA wires of one side (m), $T(t)$ is the temperature of SMA wires (K or °C), ρ is the density of SMA wires (kg/m^3) and t is the time (s).

When SMA wires are cooled, the equation describing heat transfer and temperature of SMA wires is given as:

$$\int_t h'_W \pi\, dl[T(t) - T_0]\, dt + \int_t c\rho \left(\frac{\pi d^2}{4}\right) l\, dT(t) = 0 \tag{2}$$

The equivalent heat transmission coefficient h'_W can be obtained by experiments. Simulation is carried out to the biomimetic fin used in Section 2.3 (shown in Fig. 6). The result shows that the corresponding h'_W was about 2300 W/(m^2 K). From the simulation curves we can see that in order to increase operational frequency, short pulse width with heavy electric current (or high voltage) should be supplied to SMA wires. Furthermore, SMA wire with smaller diameter could be applied to achieve higher frequency as long as the contract force is enough.

4. The design of micro-robot fish

4.1. Fish swimming mechanism

According to the momentum theorem, when fish swim by pushing water away behind them, momentum is transferred from the fish to the surrounding water and thrust is generated. Other kinds of forces acting on a swimming fish are drag, weight, buoyancy and hydrodynamic lift in the vertical direction. Swimming drag consists of viscous drag and pressure drag. Viscous drag is skin friction between the fish and the boundary layer of water, and it depends on the wetted area and swimming speed of the fish and the property of the surrounding fluid. Pressure drag is caused by distortions of flow around fish body and energy lost in the vortices formed by the fins as they generate lift or thrust.

Precision calculation of thrust is complex, so simplification by assuming steady or quasisteady flow is usually used. When a fish swim forward at a constant speed, the total thrust is equal to the total drag. On a small scale, thrust is defined as follows:

$$F_T = \frac{C_D \rho_W A V^2}{2} \tag{3}$$

Where F_T is thrust (N), C_D is drag coefficient, ρ_W is water density (kg/m^3), A is wetted surface area (m^2) and V is swimming speed (m/s).

When fish is swimming, it can narrow the wake by ensuring no vortex shed from the body but one or two vortices shed from the tail tip every fin tail beat. By doing this, reverse Karman vortex street is formed and a jet can be induced to increase thrust (shown in Fig. 7). The wake also store energy and fish can recapture energy from the vortices to enhance swimming performance and to save energy.

Two important nondimensional parameters which affect the swimming are Reynolds number (Re) and Strouhal number (St, reduced frequency). Reynolds number is the ratio of inertial over viscous forces, defined as

$$Re = \frac{LV}{\upsilon} \tag{4}$$

where L is a characteristic length (of either the fish body or the propulsor) (m), υ is the kinematic viscosity of water (m^2/s).

When Re is larger than 1000, inertial forces are dominant and viscous forces are usually neglected and when Re is smaller than 1. Viscous forces are dominant. Inertial forces and viscous forces must be both considered when Re is between 1 and 1000 [16].

Strouhal number can be approximated as

$$St = \frac{fA_{pp}}{V} \tag{5}$$

where f is tail-beat frequency (Hz) and A_{pp} is the wake width (approximately as tail-beat peak-to-peak amplitude) (m).

When St lies in the range 0.25–0.35, the swimming and thrust generation are considered as optimal.

Froude number is used to define the propulsive efficiency. It is the ratio of the useful propulsive power over the total power expended by the fish.

4.2. Structure of the micro-robot fish

Since the micro-robot fish is propelled by biomimetic fin, there are no traditional components like gears, bearings and joints. In order to activate the biomimetic fin, control circuit and batteries should be required. As a result, the micro-robot fish consists of body and biomimetic fin based propulsor (shown in Fig. 8). The micro-robot fish prototype is 146 mm in length, 17 mm in width and 34 mm in height. The weight is about 30 g. The propulsor consists of a biomimetic fin (active component) and a caudal fin (passive component). The caudal fin is used to enlarge the control surface and the thrust. *Subcarangiform* swimming can be formed by softer caudal
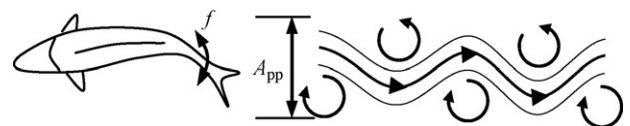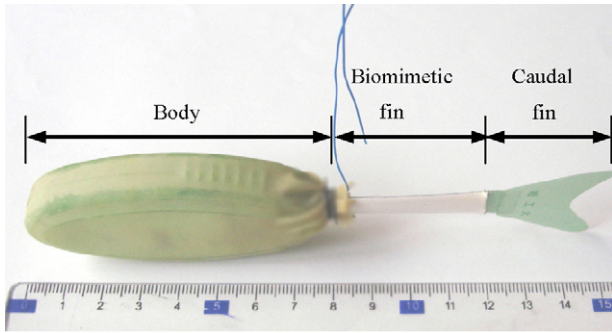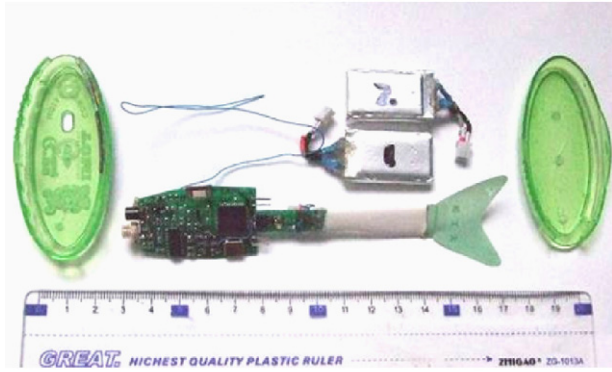

Fig. 7. The reverse Karman vortex street.

(a) After assembly

(b) Before assembly (without skin)
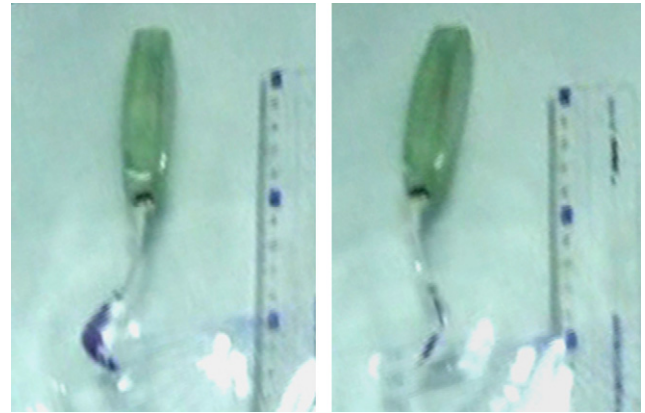
Fig. 8. Micro-robot fish prototype.

Fig. 9. *Subcarangiform*-like swimming.

in the body by shell and sealing skin. The control circuit consists of radio frequency remote control module and MCU (PIC16F877A) based open-loop driving module. The propulsor is connected to the control circuit directly.

4.3. Swimming modes

The micro-robot fish can swim forward and turn with only one biomimetic fin. When the robot fish swims forward, the biomimetic fin bend back and forth, just as illustrated in Fig. 3.

When the robot fish turns, there are three turning modes [17]:

(1) The biomimetic fin bends only to one side. The body is equivalent to a rudder and the propulsor are equivalent to a rotator of the ship. It is the most fundamental and important turning mode as the robot fish can change the turning radius and speed in this mode, and it is the simplest one.

fin while *carangiform* swimming can be obtained by harder caudal fin. To decrease the electricity value of driving the biomimetic fin and increase frequency, TiNi (50.2 at% Ni) wires with the diameter of 0.089 mm are used. In the stress-free state, the four transition temperatures are $M_f = 43.4\,^\circ$C, $M_s = 52.2\,^\circ$C, $A_s = 51.4\,^\circ$C, $A_f = 58.8\,^\circ$C. The control circuit and two 310 mAh Li-polymer batteries are enveloped

(a) Forward swimming

(b) Turning radius

(c) Speed of turning

Fig. 10. The speed of swimming forward, turning radius and speed of turning of the micro-robot fish.
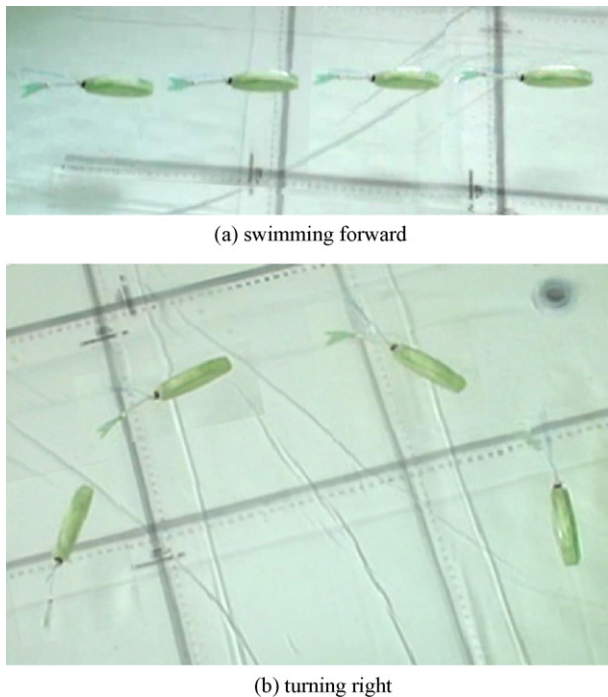
(a) swimming forward

(b) turning right

Fig. 11. Synthetic images of the status of swimming forward and turning right of micro-robot fish at 2.78 Hz, 25% duty ratio.

(2) The biomimetic fin bends to one side and keeps the posture after the robot fish swims forward at a certain speed. The robot fish turns by hydrodynamics force. Smaller turning radius can be obtained by using this mode. This mode is difficult to achieve by an open-loop control method.

(3) The biomimetic fin bends to one side rapidly from stationary state. Inertia force and friction force of the propulsor and the body are changed to the moment of rotation. Turning from a stationary state can be achieved by this turning mode. The turning radius is the smallest among the three turning modes.

5. Experiments

Swimming forward and turning capabilities were investigated. Square wave voltage was applied. Duty ratio is defined as the ratio of power on time of a period over the periodic time. Because the biomimetic fin is open-loop controlled, longer power on time means larger bending angle.

Fig. 9 shows the *subcarangiform*-like swimming status while swimming forward at a 25% duty ratio, 2.5 Hz. The average swimming speed was about 58 mm/s.

More experiments were conducted on *carangiform*-like swimming. The bending angle of the biomimetic fin increases with decreasing the driving frequency at a certain duty ratio. Turning mode (1) was applied. Prior to turning, the robot fish swam forward for 8 cycles at 25% duty ratio with the same pulse width as the turning to get an initial forward speed. Fig. 10 illustrates the speed of swimming forward and turning radius at different duty ratios and frequencies. In the case of swimming forward, a maximum frequency of 8.33 Hz was tested at a 25% duty ratio. For turning, a maximum frequency of 11.1 Hz was tested at a 33.3% duty ratio. When swimming at the same frequency, swimming speed and turning curvature (1/turing radius) of the higher duty ratio are larger than their values at lower duty ratio.

In the case of swimming forward, the peak speed at 16.7% duty ratio was obtained at 2.1 Hz, meanwhile the speed at 25% duty ratio decreased with the increase of frequency. The turning radii of both duty ratios increased firstly and then decreased with the increase of frequency. The speed of turning at 33% duty ratio decreased with the increase of frequency while at 25% duty ratio, the peak value appeared at 3.13 Hz.

A maximum speed of swimming forward of 112 mm/s was obtained at a 25% duty ratio, 2.5 Hz. A minimum turning radius of 136 mm was obtained at a 33% duty ratio, 3.7 Hz. Fig. 11 shows the status of swimming forward and turning right at a 25% duty ratio, 2.78 Hz. The Strouhal number at the maximum swimming speed was 0.58.

As the robot fish is open-loop controlled, the bending of biomimetic fin may be influenced by the water flow and the temperature inequality of water. The bending angles to each side may be different and it would result in course deviation.

6. Conclusions

A micro-robot fish propelled by a biomimetic fin is presented in this paper. The micro-robot fish has no traditional components such as gears and bearings, and it can swim noiseless and flexibly. The embedded SMA wire actuated biomimetic fin imitates the structure of squid/cuttlefish fin. Simplifications are made for the squid/cuttlefish fin to build up the biomimetic fin. The biomimetic fin consists of elastic substrate, skin, and transverse muscle-liked SMA wires. Elastic energy storage and exchange mechanism is incorporated during the bending of biomimetic fin. Initial experiments of bending were conducted to verify the concept of biomimetic fin. Thermal analysis is also applied to find proper actuation strategy. Then a radio frequency controlled micro-robot fish prototype was built based on the biomimetic fin. With different tail fin, *subcarangiform*- and *carangiform*-like swimming movements were realized. Experimental results show that the micro-robot fish can swim forward and turn with a biomimetic fin. A maximum swimming speed of 112 mm/s and a minimum turning radius of 136 mm were obtained.

Further research on the structure, material, and control strategy would be made to improve the performance of biomimetic fin. We believe that using biomimetic fin, robot fish with smaller size could be built.

Appendix A. Supplementary data

Supplementary data associated with this article can be found, in the online version, at doi:10.1016/j.sna.2008.02.013.

References

[1] M.S. Triantafyllou, G.S. Triantafyllou, An efficient swimming machine, Scientific American 272 (1995) 64–70.
[2] J. Ayers, C. Wilbur, C. Olcott, Lamprey robots, in: International Symposium on Aqua Biomechanisms, Hiratsuka, Japan, 2000, pp. 1–6.
[3] N. Shinjo, G.W. Swain, Use of a shape memory alloy for the design of an oscillatory propulsion system, IEEE Journal of Oceanic Engineering 29 (2004) 750–755.
[4] S. Guo, T. Fukuda, K. Asaka, A new type of fish-like underwater microrobot, IEEE/ASME Transactions on Mechatronics 8 (2003) 136–141.
[5] A. Punning, M. Anton, M. Kruusmaa, A. Aabloo, A biologically inspired ray-like underwater robot with electroactive polymer pectoral fins, in: International IEEE Conference on Mechatronics and Robotics 2004 (MechRob'04), Aachen, Germany, 2004, pp. 241–245.

[6] B. Kim, D.-H. Kim, J. Jung, J.-O. Park, A biomimetic undulatory tadpole robot using ionic polymer–metal composite actuators, Smart Materials and Structures 14 (2005) 1579–1585.

[7] T. Fukuda, A. Kawamoto, F. Ami, H. Matsuura, Mechanism and swimming experiment of micro mobile robot in water, in: Proc. IEEE International Conference on Robotics and Automation, New Orleans, LA, USA, 8–13 May, 1994, pp. 814–819.

[8] T. Fukuda, A. Kawamoto, F. Arai, H. Matsuura, Steering mechanism of underwater micro mobile robot, in: Proc. IEEE International Conference on Robotic and Automation, Nagoya, Japan, 21–27 May, 1995, pp. 363–368.

[9] W.M. Kier, The fin musculature of cuttlefish and squid (Mollusca, Cephalopoda) morphology and mechanics, Journal of Zoology (London) 217 (1989) 23–38.

[10] W.M. Kier, J.T. Thompson, Muscle arrangement, function and specialization in recent coleoids, Berliner Paläobiol. Abh. 3 (2003) 141–162.

[11] M.H. Dickinson, C.T. Farley, R.J. Full, M.A.R. Koehl, R. Kram, S. Lehman, How animals move: an integrative view, Science 288 (2000) 100–106.

[12] E.J. Anderson, M.E. Demont, The mechanics of locomotion in the squid *Loligo pealei*: locomotory function and unsteady hydrodynamics of the jet and intramantle pressure, The Journal of Experimental Biology 203 (2000) 2851–2863.

[13] I.K. Bartol, M.R. Patterson, R. Mann, Swimming mechanics and behavior of the shallow-water brief squid *Lolliguncula brevis*, The Journal of Experimental Biology 204 (2001) 3655–3682.

[14] G. Song, B. Kelly, B.N. Agrawal, Active position control of a shape memory alloy wire actuated composite beam, Smart Materials and Structures 9 (2000) 711–716.

[15] K. Ikuta, Micro/miniature shape memory alloy actuator, in: IEEE International Conference on Robotics and Automation, Cincinnati, OH, USA, 1990, pp. 2156–2161.

[16] C.E. Jordan, A model of rapid-start swimming at intermediate reynolds number: undulatory locomotion in the chaetognath *Sagitta elegans*, The Journal of Experimental Biology 163 (1992) 119–137.

[17] K. Hirata, Turning Modes for a Fish Robot, 2001, http://www.nmri.go.jp/eng/khirata/fish/general/turn/index_e.html.

Biographies

Zhenlong Wang graduated from the Department of Mechanical Manufacturing and Automation at Harbin Institute of Technology (HIT), Heilongjiang, China, in 2000 with a PhD. He is currently a professor in the School of Mechatronics Engineering at HIT. Professor Wang is interested in biomimetic underwater robots, non-traditional machining, micro-machining and precision machining.

Guanrong Hang received bachelor degree in Department of Mechanical Engineering and Automation at HIT, in 2003. He is currently a PhD candidate in the Department of Mechanical Manufacturing and Automation at HIT. His research interest includes studies of biomimetic underwater robots, swimming mechanics of fish, squid, and cuttlefish, and control methods of shape memory alloy.

Jian Li received bachelor degree in the Department of Mechanical Manufacturing and Automation, Shandong University, Shandong, China, in 2005. He is currently a PhD candidate in the Department of mechanical manufacture and automation at HIT.

Yangwei Wang received bachelor degree in the machine design and manufacturing and automation, Nanjing University of Aeronautics and Astronautics, Jiangsu, China, in 2002. He received MS in the Department of Mechanical Manufacturing and Automation at HIT, in 2007. He is currently a PhD candidate in the Department of Mechanical Manufacturing and Automation at HIT.

Kai Xiao received his bachelor and master degree in Department of Mechanical Manufacturing and Automation at HIT in 2002 and 2005, respectively. He is currently a PhD student in the Department of Mechanical Engineering at The Hong Kong University of Science and Technology.